

Frozen fringe explains sediment freeze-on during Heinrich events

Colin R. Meyer*¹, Alexander A. Robel², and Alan W. Rempel¹

¹Department of Earth Sciences, University of Oregon, Eugene, OR, 94703

²School of Earth & Atmospheric Sciences, Georgia Institute of Technology, , Atlanta, GA
30332

Abstract

Anomalous coarse-grained sediment layers beneath the North Atlantic likely originated from sediment freeze-on to the base of ice sheets during the last glacial period. These layers represent periods of extreme ice discharge, called Heinrich events, and are variously attributed to ice stream flow instability, ice shelf collapse, or enhanced terminus melting due to ocean warming. In this paper, we study the processes controlling how sediment freezes on to the base of ice streams and predict the volume of sediment conveyed by icebergs during a Heinrich event. The local thickness of frozen sediment is sensitive to the heat flux at the ice-bed interface and the water pressure, both of which also contribute to the controls on basal friction; as the basal water pressure increases, both the frozen sediment thickness and the basal friction decrease. The sediment discharged during a Heinrich event must have frozen on to the ice during the inter-Heinrich period. As the Heinrich event proceeds, the frozen sediment melts off the base of the ice stream, indicating that the thickness of sediments deposits in the North Atlantic may not reliably constrain Heinrich event duration. Choosing reasonable parameters corresponding to the Hudson Strait Ice Stream, our model of sediment freeze-on and discharge is consistent with observational estimates of Heinrich event sediment discharge volume.

This paper is a postprint of a peer-reviewed manuscript published in *Earth and Planetary Science Letters* with the doi: [10.1016/j.epsl.2019.115725](https://doi.org/10.1016/j.epsl.2019.115725).

*colinmeyer@gmail.com

1 Introduction

During the last glacial period, massive sediment-laden armadas of icebergs were periodically discharged from the Northern Hemisphere ice sheets, after which they melted and deposited coarse-grained sediment throughout the North Atlantic. Originating from fast-flowing ice streams of Northern Hemisphere ice sheets (e.g. Laurentide, Fennoscandian, British), the 5-10 kyr periodicity of these sediment layers indicates a corresponding periodicity in the discharge from these ice streams, with a long quiescent phase interrupted by a short active phase that begets the ice-rafted debris observed in the North Atlantic ocean sediments. The active period in ice stream discharge and the sediment layers produced are known as Heinrich events (Heinrich, 1988; Hemming, 2004).

Heinrich events offer a unique view into the dynamics of past ice sheets — coupling climate, ocean, and ice sheet processes. In this way, studying Heinrich events may also shed light on the dynamics of present ice sheets, exemplified by the observations of stagnation/reactivation in Antarctic ice streams on multi-centennial timescales (Hulbe and Fahnestock, 2007; Catania et al., 2012; Mantelli et al., 2016). On the longer timescales of Heinrich events, stagnation/reactivation occurs due to snow accumulation, basal warming from frictional heat, and increased lubrication from basal meltwater decreasing the sliding friction. This mechanism for Heinrich events has alternately been referred to as the ‘binge–purge’ or thermal oscillation hypothesis (MacAyeal, 1993a,b; Fowler and Schiavi, 1998; Robel et al., 2013). The timing of Heinrich events is notable in that they coincide with periods of relatively cold temperatures in the Northern Hemisphere due to Milankovitch forcing and are not clearly correlated with Dansgaard-Oeschger events (Ziemen et al., 2019). Therefore, it is difficult to implicate the atmosphere in driving Heinrich events. The timing of the Heinrich layers does, however, correlate with changes in the Atlantic Ocean overturning circulation (Alvarez-Solas et al., 2010, 2011, 2013), which may trigger Heinrich events either by disintegrating ice shelves (Hulbe, 1997; Hulbe et al., 2004; Marcott et al., 2011) or by warm water overtopping a sill generated by isostatic rebound of the earth (Bassis et al., 2017).

In addition to the ice-rafted debris, there is strong climatic evidence for large volumes of ice being discharged during Heinrich events (Broecker, 1994; Ganopolski and Rahmstorf, 2001; Hemming, 2004). The ice-rafted debris layers within ocean sediments indicates that large volumes of sediment were carried by calved icebergs. Yet fast ice stream flow is not a favorable regime in which to freeze on sediment: friction and geothermal heat cause the base of the ice stream to melt and, as we show here, the water pressure would be too high to overcome porescale surface energy, which acts to prevent the ice from infiltrating into basal sediments. It has long been known (e.g. Alley and MacAyeal, 1994) that there is a paradox inherent in maintaining sediment frozen at the base of an ice stream at the same time that rapid ice stream flow produces high volumes of sediment discharge during Heinrich events. The prevailing conceptual solution to this paradox (Alley and MacAyeal, 1994) is that sediment must be stored during the inter-Heinrich period. However, the physical mechanism of this storage is not well understood.

While numerous models exist to describe the extreme discharge of ice during Heinrich events, there is a gap in understanding of how sediment freezes on to the base of an ice stream given the elevated melt rates and water pressures. In this paper, we study the process by which frozen sediment attaches to the base of glaciers using a thermomechanical treatment derived from first principles and verified experimentally (Rempel et al., 2004; Rempel, 2007, 2008). Modifying the binge–purge formulation developed by Robel et al. (2013), we include these new physics of sediment freeze-on while maintaining a framework that could be applied to any ice sheet model, including models that contain the other mechanisms for Heinrich events, i.e. ice shelf collapse or ocean warming. The combination of binge–purge and sediment freeze-on models allows us to simulate Heinrich events as long-period oscillations in ice stream velocity, which pick up and discharge sediment-laden ice. Our model produces a theoretical prediction for the timing and volume of sediment discharge during a Heinrich event.

This paper is organized as follows: first, we describe the physics of subglacial freeze-on. Then, we couple freeze-on to the Robel et al. (2013) formulation of the binge–purge model. We follow our model description with a section showing our results for the timing and volume of sediment discharged in a Heinrich event, which we discuss in the context of observational estimates of Heinrich event sediment discharge, leading to a brief conclusion section.

2 Model

2.1 Frozen fringe thermomechanics

The conservation of mass, momentum, and energy at the basal interface between ice and sediment are manifestations of macroscopic ice stream features such as the ice thickness, basal velocity, and temperature profile. At the base of ice streams underlain by porous sediments, ice can infiltrate into the sediments if the pore water pressure is low enough within the sediment interstices (Rempel, 2007, 2008; Meyer et al., 2018) by the same process that gives rise to frost heave in subaerial environments (O’Neill and Miller, 1985; Fowler and Krantz, 1994; Rempel, 2010). In this section, we describe the theory for how ice infiltrates into sediments and forms what is known as a frozen fringe, which is named as an analogy to the capillary fringe in vadose zone hydrology (Rempel, 2012).

The two primary quantities that control the infiltration of ice into a given sediment (i.e. initiation of a frozen fringe) are the basal melt rate \dot{m} and the effective pressure N , which itself determines the state of consolidation and thereby modulates the porosity, ϕ . Considering the energy balance at the base of an ice stream, the sources of heat are geothermal Q_g and frictional Q_f while heat is carried away by conduction into the overlying ice Q_b . Thus, the melt rate \dot{m} is given as

$$\rho_i \mathcal{L} \dot{m} = Q_g + Q_f - Q_b, \quad (1)$$

where ρ_i is the ice density and \mathcal{L} is the specific latent heat. Although the geothermal heat flux can be considered a fixed parameter, the frictional and basal heat fluxes are dependent on ice stream evolution, which we calculate from the ice stream evolution model of Robel et al. (2013), and these heat fluxes would likely be different for another choice of ice sheet model.

The force balance at the basal interface is paramount in determining whether ice can infiltrate into the subglacial sediment. The deficit between the overburden pressure σ_o from the weight of overlying ice and the water pressure p_w is referred to as the effective pressure N , i.e.

$$N = \sigma_o - p_w, \quad (2)$$

and it represents the load carried by grain contacts within the sediment skeleton. The shear stress at the basal interface τ_b is related to the effective pressure through the Mohr-Coulomb relationship, given by

$$\tau_b = \mu N, \quad (3)$$

where μ is the coefficient of friction (having neglected cohesion; Iverson et al., 1998; Minchew et al., 2016). In this way, the effective pressure sets the sediment yield stress, which is the primary restraint to glacier motion and controls the ice velocity, thus, Heinrich event initiation.

2.1.1 Premelting and ice infiltration

At the microscopic scale, the interface between the ice and sediments is not flat. Rather, the ice conforms to the sediment surface with a thin layer of premelted water separating the ice and sediment particles (figure 1a; Rempel, 2008). Irrespective of whether the interface is at or far below the pressure melting temperature, premelted water can achieve an equilibrium with the ice and adjacent sediment particles due to quantum dipole moment fluctuations and other microphysical processes (Dash et al., 2006). The intermolecular interactions that cause premelting allow forces to be transferred between the ice and sediment grains, enabling the ice pressure to exceed the water pressure. In other words, the water can remain liquid at temperatures far below the bulk melting temperature while in contact with the ice because it is at a different pressure, i.e. $N > 0$, due to premelting (Meyer et al., 2018; Rempel and Meyer, 2019). Across the thin layer of premelted water that separates the ice and sediment grains, the disjoining force repels the ice from the sediment grains and transfers the effective pressure load deficit onto the sediment skeleton (figure 1a).

As the effective pressure increases, the premelted films on top of sediment particles thin and the ice curves into the interstitial pore space. At a critical effective pressure p_f set by the surface energy γ_{iw} and the radius of curvature of the interstitial pore throats r_p , the ice can infiltrate into the sediments and generate a frozen fringe (figure 1b), where the critical effective pressure is given as

$$p_f = \frac{2\gamma_{iw}}{r_p}. \quad (4)$$

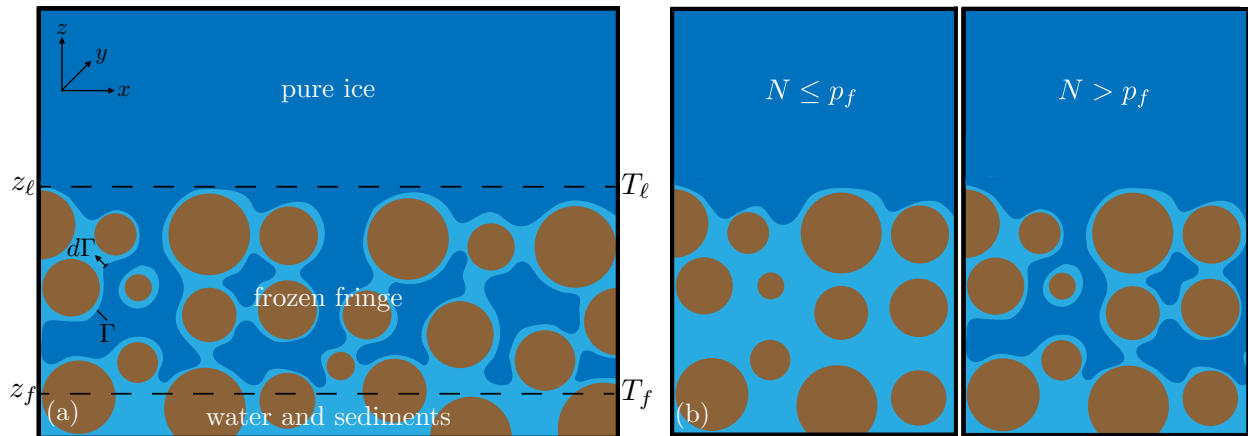


Figure 1: Schematic of a frozen fringe: (a) The partially saturated frozen fringe sits between pure ice and unfrozen till. The temperature T_f at the bottom of the fringe z_f is greater than the temperature T_ℓ at the top of the fringe $z_\ell = z_f + h$, where h is the fringe thickness. (b) Force balance dictates that the effective pressure N must be greater than p_f for a fringe to form.

95 For micron sized pore throats and $\gamma_{iw} = 0.034$ N/m, the entry pressure is $p_f \sim 70$ kPa (Rempel, 2008; Meyer et al., 2018; Lipovsky et al., 2019).

The ice that enters the pore space to form a frozen fringe partially saturates the available porosity, meaning that there is both water and ice between sediment grains. Accordingly, for a given control volume, the total fringe density ρ_f is partitioned as

$$\rho_f = (1 - \phi)\rho_s + \phi S\rho_i + \phi(1 - S)\rho_w, \quad (5)$$

100 where ϕ is the porosity, S is the ice saturation, ρ_s , ρ_i , and ρ_w are the sediment, ice, and water densities respectively (e.g. Meyer and Hewitt, 2017). The ice saturation is the fraction of the pore space occupied by ice and varies within the fringe as a function of temperature. The temperature at the bottom of the fringe T_f is set by curvature and premelting as

$$T_f = T_m - \frac{p_f T_m}{\rho_i \mathcal{L}}, \quad (6)$$

105 which is below the bulk melting temperature T_m that is described by the generalized Clapeyron relation, consistent with the Gibbs-Thomson effect (Worster, 2000; Dash et al., 2006; Rempel, 2008). The temperature at the top of the fringe T_ℓ is set by the force, heat, and mass balance constraints described below. The saturation within a frozen fringe is then empirically described by

$$S = 1 - \left(\frac{T_m - T_f}{T_m - T} \right)^\beta, \quad (7)$$

110 where the exponent β has been tabulated (Andersland and Ladanyi, 2004). Additionally, equation (7) ensures that the saturation is zero at the bottom of the fringe where $T = T_f$, while a finite jump in saturation to $S = 1$ takes place at the top of the fringe.

Water flow through the interstices and along the thin films within the fringe can be model with Darcy's law. The permeability of the fringe to water flow depends on the saturation, and therefore, the temperature structure. An empirical relationship for the permeability k is given as

$$k = k_0 \left(\frac{T_m - T_f}{T_m - T} \right)^\alpha, \quad (8)$$

115 where the exponent α has also been tabulated (Andersland and Ladanyi, 2004) and k conforms to the permeability k_0 of the sediments beneath the fringe (Rempel, 2008).

2.1.2 Heave rate of a frozen fringe

Across the liquid layers that separate ice and till, there are disjoining forces between all interstitial ice grains and sediment particles. The combined effect of all of these forces, gives rise to the heave force that is responsible for vertical displacement in frost heave (Rempel et al., 2001, 2004) and a heave rate V , which is given as

$$V = \frac{\frac{\rho_i \mathcal{L}}{T_m} \left(T_m - T_\ell + \phi \int_{T_f}^{T_\ell} S dT \right) - N}{\frac{\rho_i^2 \eta}{\rho_\ell^2} \int_{z_f}^{z_\ell} \frac{(1-\phi S)^2}{k} dz + \frac{\eta R^2}{d^3}}, \quad (9)$$

where we have neglected gravitational effects in the fringe, η is the viscosity of water (which to a good approximation is independent of temperature and film thickness), R is the sediment grain size, and d is the thickness of the premelted films coating these grains (Rempel and Worster, 1999; Wettlaufer and Worster, 2006; Rempel, 2008). The first term in the numerator is the pressure exerted by the sediment particles on the ice and the second term is the effective pressure. The denominator is a combination of water-flow permeability and thin film flow resistance at the fringe–glacier contact z_ℓ , which we treat approximately using a single characteristic R while neglecting variations in d with temperature.

To solve for the heave rate V we need to determine the temperature distribution within the fringe. In general, this involves solving a transient, free-boundary, second-order partial differential equation for temperature (Rempel, 2007, 2008). Instead, we make a common approximation and treat the temperature distribution within the fringe as linear (Fowler and Krantz, 1994; Rempel, 2008; Anderson and Worster, 2014), i.e.

$$T = T_f + (T_\ell - T_f) \left(\frac{z - z_f}{z_\ell - z_f} \right). \quad (10)$$

Based on this solution, we define the fringe thickness as $h = z_\ell - z_f$ and the temperature gradient G as

$$G = -\frac{T_f - T_\ell}{h} = -\frac{Q_g + Q_f}{K}, \quad (11)$$

where K is the thermal conductivity. The temperature gradient is a negative quantity since $T_f > T_\ell$, i.e. the bottom of the fringe is warmer than the top of the fringe (cf. figure 1). The amount of undercooling at the top of the fringe can be nondimensionally quantified as

$$\theta_\ell = \frac{T_m - T_\ell}{T_m - T_f} = 1 - \frac{Gh}{T_m - T_f}, \quad (12)$$

where θ_ℓ is unity for a nascent fringe and grows with the size of the fringe.

Using the linear temperature profile and the dimensionless undercooling, along with the constitutive behavior from equations (7) and (8), we can evaluate equation (9) and determine the rate of heave as

$$V = V^* \frac{\theta_\ell + \phi \left[1 - \theta_\ell + \frac{1}{1-\beta} \left(\theta_\ell^{1-\beta} - 1 \right) \right] - \frac{N}{p_f}}{\frac{(1-\phi)^2}{\alpha+1} \left(\theta_\ell^{\alpha+1} - 1 \right) + \frac{2(1-\phi)\phi}{\alpha-\beta+1} \left(\theta_\ell^{\alpha-\beta+1} - 1 \right) + \frac{\phi^2}{\alpha-2\beta+1} \left(\theta_\ell^{\alpha-2\beta+1} - 1 \right) + \Pi}, \quad (13)$$

where V^* and Π are defined as

$$V^* = -\frac{\rho_\ell^2 \mathcal{L} G k_0}{\rho_i T_m \eta}, \quad (14a)$$

$$\Pi = -\frac{\rho_\ell^2 k_0 G R^2}{\rho_i^2 (T_m - T_f) d^3}. \quad (14b)$$

These quantities can be thought of as the nominal heave rate V^* and liquid flow resistance around a sediment grain relative to the permeable flow resistance through the fringe Π . Thus, from equation (13) and the parameters in table 1, we can calculate the heave rate for a given fringe thickness, effective pressure, and heat fluxes.

ρ_i	920 kg m ⁻³	γ_{iw}	0.034 J m ⁻²
ρ_w	1000 kg m ⁻³	η	1.8×10^{-3} Pa s
ρ_s	2650 kg m ⁻³	r_p	10^{-6} m
R	4×10^{-5} m	α	3.1
K	2 kg m s ⁻³ K ⁻¹	β	1.3
\mathcal{L}	3.34×10^5 m ² s ⁻²	μ	0.6
d	10^{-8} m	a	1.41×10^5 Pa
Q_g	0.050 W m ⁻²	b	21.7
T_m	273 K	p_f	6.8×10^4 Pa
k_0	4.1×10^{-17} m ²	w	90×10^3 m

Table 1: Table of parameters for frozen fringe model and Heinrich event calculations.

145 2.1.3 Time evolution of a frozen fringe

To determine the transient evolution of the fringe, we again treat the temperature distribution within the fringe as linear and evaluate an approximate heat balance across the fringe. While heat is lost from the fringe into the overlying ice, heat enters the fringe by frictional and geothermal heat flux; any imbalance determines the melt rate \dot{m} . Changes in phase between the water and ice also take place within the fringe, so that the combination of heaving and fringe growth (Rempel, 2008) required for mass balance imply that

$$\phi \bar{S} \frac{dh}{dt} = -\dot{m} - V, \quad (15)$$

where \bar{S} is the average saturation within the fringe, given by $\bar{S} = 1 - \theta_\ell^{-\beta}$, and the heave rate V is a function of the fringe thickness h , the effective pressure N , and sediment characteristics through equation (13). Thus, for a given initial fringe thickness and known \dot{m} , N , and ϕ , equation (15) allows us to determine the thickness of the frozen fringe at the base of an ice stream as a function of time (e.g. figures 2b and 3).

155 In an earlier effort to derive estimates of discharged sediments during a Heinrich event, Alley and MacAyeal (1994) use a similar equation to (15) with several key differences. First, and foremost, they do not consider the effect of heave (i.e. $V = 0$ in their formulation) meaning that fluid transport and force balance are not accounted for in determining the thickness of basal freeze on. This assumption is problematic because it means that there is no steady state for the basal interface at any non-zero melt rate. In other words, the assumptions of $V = 0$ in Alley and MacAyeal (1994) imply that a glacier must always be freezing sediment on at the base, redepositing it, or simply producing meltwater. In our work, a fringe can maintain a steady state when the heave rate balances the freezing rate $V = -\dot{m}$. Additionally, Alley and MacAyeal (1994) do not account for the porous nature of sediments and instead allow ice to freeze with full saturation and a porosity of unity, much like growing ice on a lake. This is a recognized shortcoming to their work (Alley et al., 1997) and notably different from the simple “freeze” case we make use of for comparison below, which is formulated to represent freezing into an idealized porous half-space (i.e. $\bar{S} = 1$, $V = 0$).

170 The challenge of implementing equation (15) is that during a Heinrich event the fringe melts away. Without a fringe, the heave rate must reduce to a force balance condition, which determines the temperature at the base of the ice stream, and must be warmer than the fringe entry temperature T_f (cf. equation (6)). Accordingly, we model the behavior when $h = 0$ and $0 \leq \theta_\ell \leq 1$ by replacing equation (13) with

$$V = -\dot{m} = \frac{V^*}{\Pi} \left(\theta_\ell - \frac{N}{p_f} \right). \quad (16)$$

Once the ice stream base cools below T_f , and the effective pressure is larger than p_f , the fringe can regrow.

2.2 Ice stream forcing and frozen fringe coupling

In this section we describe the coupling between frozen fringe evolution and ice stream dynamics. While there are many competing theories for the precise mechanism behind Heinrich events, fast ice stream or ice sheet discharge is a feature of all of these models, regardless of whether the mechanism of initiating fast flow

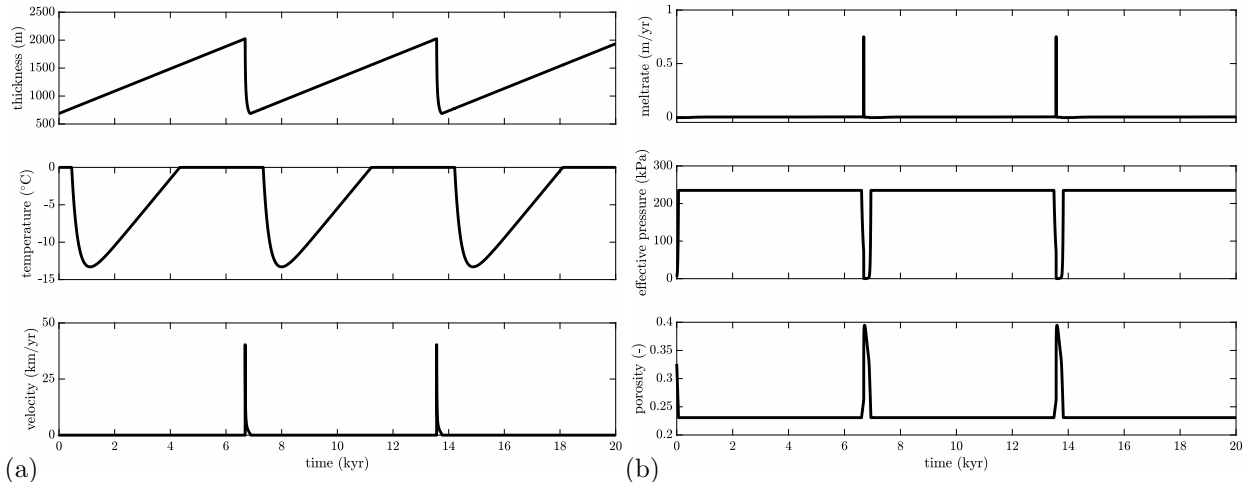


Figure 2: Robel et al. (2013) binge-purge mechanism for Heinrich events: (a) as the ice stream thickens (top), the basal temperature increases (middle), causing the basal friction to decrease, and leading to an extreme spike in velocity (bottom). (b) as the Heinrich event starts, the melt rate peaks (top), the effective pressure drops (middle), and the sediment porosity spikes (bottom).

is external or internal to the ice sheet. Here we focus on understanding the manner in which sediment is picked up by the ice stream and subsequently discharged, yet the physics of basal freeze-on described in the previous section is general enough such that it could be implemented in any ice sheet model that calculates basal melt rate and effective pressure. To facilitate comparison with Alley and MacAyeal (1994), we use the ice stream thermal oscillation model of Robel et al. (2013), which builds off of the binge-purge formulation of MacAyeal (1993a,b) and the basal strength treatment of Tulaczyk et al. (2000a). The mathematical details of this model are described in Robel et al. (2013), so the discussion herein will be brief.

The ice stream model is forced by prescribed temperature and accumulation rate at the ice stream surface and geothermal heat flux at the bed, which results in two primary ice stream behaviors: steady streaming, and thermal oscillations. The thermal oscillations can produce fluctuations in ice discharge over a range of amplitudes, including a range with similar characteristics to Heinrich events (Robel et al., 2013). Here we focus on large-amplitude thermal oscillations, which are characterized by a quiescent inter-Heinrich period of slow velocity and a short-duration extreme discharge event. A typical sequence of Heinrich event cycles is displayed in figure 2a, where the top panel shows the ice stream thickness, the middle panel shows the basal temperature, and the bottom panel shows the ice stream velocity. The accumulation rate is 0.2 m/yr and the ice surface temperature is -35°C . Thus, figure 2a demonstrates the binge-purge mechanism for Heinrich events: as the ice stream thickens (binge), conductive heat transport through the ice diminishes and the basal temperature warms up to the melting temperature, enabling sediment failure and ice stream flow. The added heat from friction warms the base even more, allowing the ice stream to flow faster (purge) until the reservoir of ice upstream is exhausted, causing the ice stream base to freeze and ice flow to stop. The cycle then repeats. The interaction between the overlying ice stream and the sediments below plays an important role in the initiation of Heinrich events. Especially important is the connection between the approach of the basal temperature towards the melting point and rate of ice stream flow. Robel et al. (2013) connect the thermodynamics and ice flow mechanics through a till-dilation hydrology model, where the effective pressure is determined from the amount of meltwater present in sediments. Coulomb friction, i.e. equation (3), then determines the basal shear stress (cf. figure 2b). In this formulation, net melting at the base of the ice stream produces meltwater that infiltrates into the sediments. Following the experiments of Tulaczyk et al. (2000b,a), the water is accommodated in the sediments by increasing the void space (i.e. an undrained plastic bed), as determined by the void ratio e , which is the volume fraction of voids relative to solids in a representative control volume. The sediment porosity ϕ is related to the void ratio as $\phi = e/(1 + e)$. The experimentally determined empirical relationship between the void ratio and effective pressure is given as

$$N = ae^{-b(e-e_c)}, \quad (17)$$

where a and b are empirical, and e_c is the till consolidation threshold, which is typically treated as a lower bound on the void ratio. This critical void ratio e_c is an important parameter in the model of Robel et al. (2013), because it controls the strength of the ice stream bed during inter-Heinrich quiescent periods, thereby controlling the onset of a Heinrich event.

Equation (17) is related to the initiation of a frozen fringe described in section 2.1.1, where ice can infiltrate into sediments when the effective pressure exceeds a threshold stress $p_f = 2\gamma_{iw}/r_p$. However, if e_c represents the void ratio when $N = p_f = a$, as proposed in Robel et al. (2013), then it is inconsistent to also treat it as a lower bound on the void ratio, since that would imply that the effective pressure would never be larger than p_f and no sediment could freeze on to the base of the ice stream. Accordingly, here we instead assume that the till will yield beneath the relatively stiff frozen fringe (Moore, 2014), which is the ‘rigid-ice’ model of O’Neill and Miller (1985), and that equation (17) holds for the ice-free till beneath the ice stream both with and without a frozen fringe. In other words, we treat a , b , and e_c as experimentally constrained free parameters and assume that equation (17) always determines the effective pressure.

With this assumption in mind, the fringe thickness as a function of time can then be calculated *diagnostically* from the output of the Robel et al. (2013) Heinrich event simulations using equation (15), which is what we do in the next section (cf. figure 2b). Before closing, however, it is important to note that equation (17) is a specific choice of hydrology model and sliding law, yet the formulation resulting in equation (15) is sufficiently general that any other specifications of N , \dot{m} , and ϕ would work equally well (e.g., Hewitt, 2013; Werder et al., 2013).

3 Results and discussion

In this section, we use the output of the Robel et al. (2013) model coupled to our description of sediment freeze-on to predict the amount of sediment discharged during a Heinrich event. In this way, we model the periodic discharge of large icebergs with sediment frozen to their base, using parameters representing the Hudson Strait Ice Stream and underlying geology. We assume that the sediment is infinitely deep, which is reasonable given that at most tens of meters are evacuated and the sediment underneath the Laurentide Ice Sheet was likely many 100s of meters thick (Laske and Masters, 1997). We treat the flux of ice from the ice stream into the ocean as equivalent to the rate of iceberg production, i.e. we neglect substantial ocean melting at the ice stream terminus (Wagner et al., 2018). This is reasonable because significant ocean melting prior to calving would ablate the frozen basal sediment, removing any ice-rafted debris very close to the ice-ocean interface, which is inconsistent with observations (Alley and MacAyeal, 1994; Hulbe, 1997).

To determine the heave rate and fringe thickness as a function of time, we adopt the Robel et al. (2013) effective pressure, melt rate, and porosity model outputs displayed in figure 2 and insert them into equations (13) and (15). The result of integrating equation (15) is shown as the brown line in figure 3a. We compare the fringe thickness (brown line) to the freezing of porous sediment without heave (i.e. dashed green line in figure 3; $\bar{S} = 1$, $V = 0$ in equation (15)). While the shapes of the sediment thickness and flux curves are similar, the consequential difference is that the frozen fringe entirely disappears during the Heinrich event in the presence of heave (brown line). The disappearance of fringe during Heinrich events results in two significant features with important implications for interpreting ice-rafted debris layers in ocean sediment cores. First, the fringe disappearing means that the Heinrich layer thickness does not reliably determine the duration of a Heinrich event. In other words, just because an ice stream stopped discharging sediment does not mean that the period of extreme ice discharge has ceased, rather it could just mean that the fringe has melted out from the basal ice layer near the ice stream grounding line. Second, the flux of sediment out of the ice stream is consistently much lower for the fringe when compared to the porous freezing model, as shown in figures 3b for the flux and 3c for the cumulative sediment discharged. Here the flux is the frozen sediment thickness multiplied by the ice stream velocity and the ice stream width w . The cumulative discharge is the integral of the flux with time.

The fact that the fringe disappears during the Heinrich event is due to the low effective pressure and high melt rate consistent with fast ice velocity (cf. figures 2 and 3). The high pore water pressure and frictional heat combine to rapidly lower the fringe thickness. The water pressure is too high during the Heinrich event to overcome porescale surface energy (equation (4)) and the local melting temperature warms as the difference between ice and water pressures decreases (Rempel and Meyer, 2019). Simultaneously, the

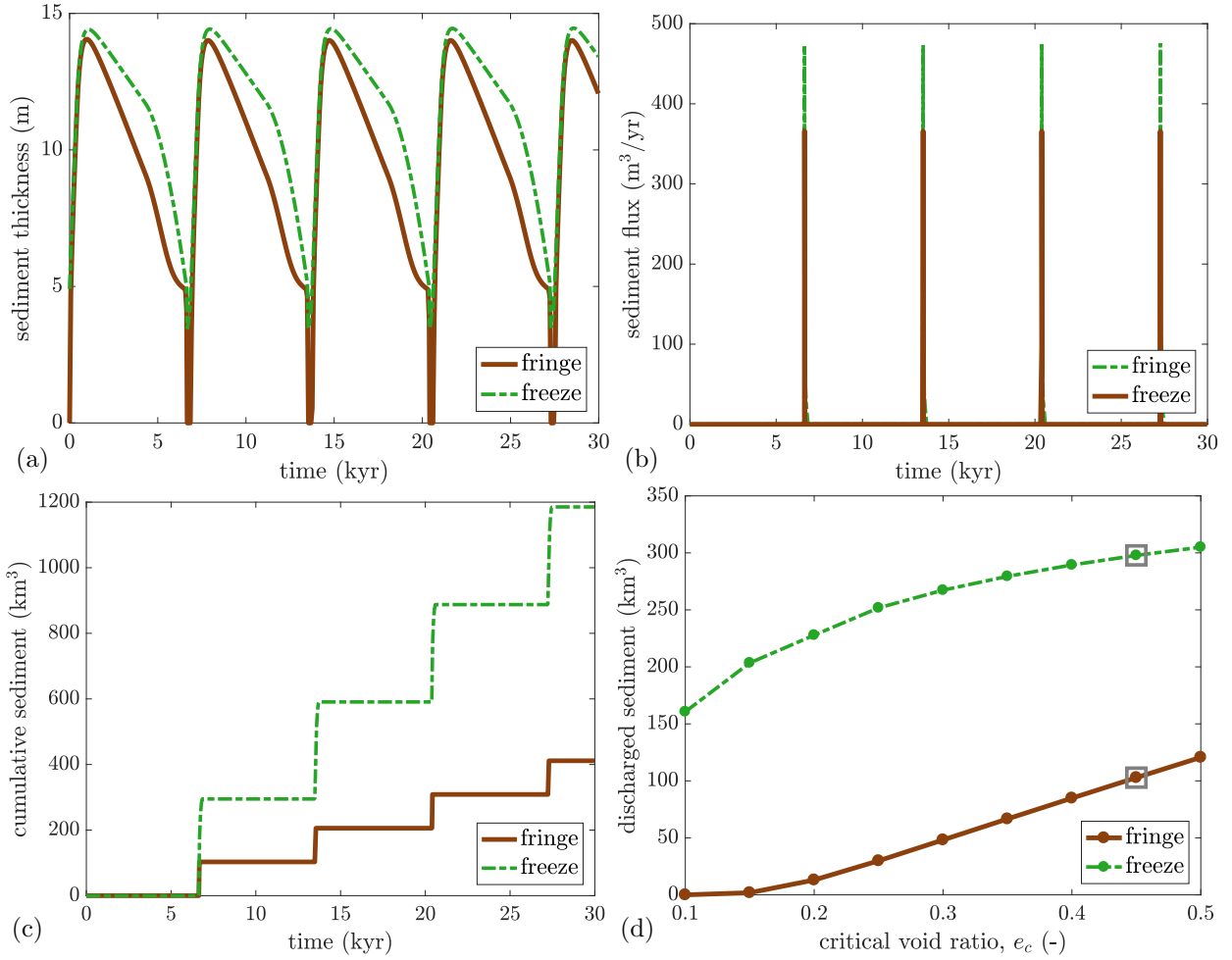


Figure 3: Results for spatially lumped model: (a) fringe and porous freeze-on thicknesses as a function of time and many Heinrich events. (b) flux of sediment discharged during a Heinrich event, calculated as the sediment thickness times the velocity times the width of the ice stream w . (c) cumulative sediment discharged, which is the integral of the sediment flux in time. (d) The total discharged sediment per Heinrich event as a function of the parameter e_c . The gray square indicates the value used for (a)-(c).

addition of frictional heat causes the fringe to melt directly following equation (15). Our model corroborates Alley and MacAyeal (1994) in showing that the frozen sediment builds up during the inter-Heinrich period and then is melted off during the Heinrich event. Moreover, since the frozen sediment melts off the base of the ice stream during each Heinrich event, the amount of sediment discharged is determined by the freeze-on sediment thickness at the end of the inter-Heinrich period and *not* the duration of the Heinrich event. The difference between the duration of sediment discharge and fast ice flow has implication for reconstructing ice discharge from sediment cores. This difference states that the oceanic ice-rafted debris layer thickness will only record the sediment discharge period, indicating that fast ice flow could have prevailed for a longer period of time while maintaining the same sediment discharge signature.

The differences in cumulative discharge between the fringe and the porous freezing case are interesting in terms of magnitude. These simulations represent the sediment discharged for a single ice stream and for each Heinrich event in this cycle the porous freezing model gives about 300 km³ of discharged sediment, whereas the fringe case only produces about 100 km³. From a compilation of multiple sediment cores, Hemming (2004) (table 5) estimate that the total Heinrich event sediment discharge is between 100 and 300 km³ for *all* ice streams involved in Heinrich events. For the meltrates given by the Robel et al. (2013) model, the porous freezing results (dashed green lines) are difficult to reconcile with estimates of sediment volume for all Heinrich events, which include total discharge of about about 100 km³ during H1 and H3. Conversely, the fringe model *is* consistent with a single ice stream source for these smaller Heinrich events, and can simultaneously explain larger Heinrich events with a contribution from multiple ice stream sources, which has some support from geochemical provenance studies (Hemming, 2004).

The results show in figure 3(a)-(c) are for a specific choice of parameters. While we have used representative values, the actual parameter values are uncertain. One such uncertain parameter is the critical void ratio e_c . To understand how the results change with e_c , we vary it over a reasonable range and determine the amount of sediment discharged (cf. figure 3d). Sediment discharge increases monotonically with e_c because the effective pressure also increases with e_c (for fixed a and b). If the threshold pressure p_f is held constant and the effective pressure increases, the thickness of the frozen sediment layer also increases (Rempel, 2008; Meyer et al., 2018).

The spatially lumped model predicts that sediment is discharged at the beginning of a Heinrich event and then the fringe melts off, but it does not capture how this occurs along the direction of flow within an ice stream. If the effective pressure, melt rate, and porosity were constant along the central flowline of an ice stream, then these results would be easy to extrapolate, but such uniformity is unlikely to hold. Due to variations in effective pressure, melt rate, and porosity, we expect the fringe thickness to vary along an ice stream. Therefore, it is plausible that the advection of frozen sediment may play a role in ice streams discharging sediment. In the spatially lumped model, the advection of sediment is implicit, i.e. the variation of fringe thickness along the ice stream is accounted for in a length-averaged sense. It is likely that sediment advection along an ice stream is the mechanism by which sediment makes it to the front of an ice stream to be calved off and carried away by icebergs. To accommodate the downstream advection of frozen fringe, we could assume that slip occurs at the base of the frozen fringe (Rempel, 2008; Moore, 2014; Meyer et al., 2018) and modify equation (15) to advected fringe along a flowline as

$$\phi \bar{S} \left(\frac{\partial h}{\partial t} + U \frac{\partial h}{\partial x} \right) = -\dot{m} - V, \quad (18)$$

where U is the ice stream velocity and x is the along-flow coordinate. However, since it would likely only quantitatively, but perhaps not qualitatively affect the results reported in this section, we leave this for future work.

4 Conclusions

In this paper, we describe the physics of how sediment is frozen on to the base of ice streams during Heinrich events. Our model is based on the thermodynamically consistent, experimentally verified models that have been developed for frost heaving soils. The important additional ingredient in our model over prior treatments is coupling thermodynamics at the phase change boundary and force balance. When applied to a spatially lumped binge-purge type model for Heinrich events, we find that the frozen fringe produces on the

order of 100 km^3 of sediment per Heinrich event. The amount of sediment discharged in a porous freezing model, which does not account for wetting processes or force balance, is on the order of 300 km^3 . The fact that the fringe model produces less discharged sediment corroborates the idea that multiple ice streams may contribute to a single Heinrich layer, yet also produces enough sediment to explain the smaller Heinrich events from a single ice stream source. Our model also shows that the frozen sediments melt off during the period of fast ice stream flow and therefore, the duration of sediment discharge is not necessarily equivalent to the duration of fast ice flow.

5 Acknowledgments

We thank Christian Schoof, Gwenn Flowers, Richard Hindmarsh and Doug MacAyeal for discussions and acknowledge financial support from NSF-1603907.

References

References

- R. B. Alley and D. R. MacAyeal. Ice-rafted debris associated with binge/purge oscillations of the Laurentide Ice Sheet. *Paleoceanogr. Paleoclimatol.*, 9(4):503–511, 1994. doi: 10.1029/94PA01008.
- R. B. Alley, K. M. Cuffey, E. B. Evenson, J. C. Strasser, D. E. Lawson, and G. J. Larson. How glaciers entrain and transport basal sediment: physical constraints. *Quat. Sci. Rev.*, 16(9):1017–1038, 1997. doi: 10.1016/S0277-3791(97)00034-6.
- J. Alvarez-Solas, S. Charbit, C. Ritz, D. Paillard, G. Ramstein, and C. Dumas. Links between ocean temperature and iceberg discharge during Heinrich events. *Nat. Geosci.*, 3:122–126, 2010. doi: 10.1038/NGEO752.
- J. Alvarez-Solas, M. Montoya, C. Ritz, G. Ramstein, S. Charbit, C. Dumas, K. Nisancioglu, T. Dokken, and A. Ganopolski. Heinrich event 1: an example of dynamical ice-sheet reaction to oceanic changes. *Clim. Past*, 7:1297–1306, 2011. doi: 10.5194/cp-7-1297-2011.
- J. Alvarez-Solas, A. Robinson, M. Montoya, and C. Ritz. Iceberg discharges of the last glacial period driven by oceanic circulation changes. *Proc. Natl. Acad. Sci.*, 110(41):16350–16354, 2013. doi: 10.1073/pnas.1306622110.
- O. B. Andersland and B. Ladanyi. *Frozen ground engineering*. John Wiley & Sons, Somerset, 2004.
- A. M. Anderson and M. G. Worster. Freezing colloidal suspensions: periodic ice lenses and compaction. *J. Fluid Mech.*, 758:786–808, 2014. doi: 10.1017/jfm.2014.500.
- J. N. Bassis, S. V. Petersen, and L. M. Cathles. Heinrich events triggered by ocean forcing and modulated by isostatic adjustment. *Nature*, 542:332–334, 2017. doi: 10.1038/nature21069.
- W. S. Broecker. Massive iceberg discharges as triggers for global climate change. *Nature*, 372(6505):421, 1994. doi: 10.1038/372421a0.
- G. Catania, C. L. Hulbe, H. Conway, T. A. Scambos, and C. F. Raymond. Variability in the mass flux of the ross ice streams, West Antarctica, over the last millennium. *J. Glaciol.*, 58(210):741–752, 2012. doi: 10.3189/2012JoG11J219.
- J. G. Dash, A. W. Rempel, and J. S. Wettlaufer. The physics of premelted ice and its geophysical consequences. *Rev. Mod. Phys.*, 78(3):695, 2006. doi: 10.1103/RevModPhys.78.695.
- A. C. Fowler and W. B. Krantz. A generalized secondary frost heave model. *SIAM J. Appl. Math.*, 54(6):1650–1675, 1994. doi: 10.1137/S0036139993252554.

- A. C. Fowler and E. Schiavi. A theory of ice-sheet surges. *J. Glaciol.*, 44(146):104–118, 1998. doi: 10.3189/S0022143000002409.
- A. Ganopolski and S. Rahmstorf. Rapid changes of glacial climate simulated in a coupled climate model. *Nature*, 409(6817):153, 2001. doi: 10.1038/35051500.
- 350 H. Heinrich. Origin and consequences of cyclic ice rafting in the Northeast Atlantic Ocean during the past 130,000 years. *Quat. Res.*, 29(2):142 – 152, 1988. ISSN 0033-5894. doi: 10.1016/0033-5894(88)90057-9.
- S. R. Hemming. Heinrich events: Massive late pleistocene detritus layers of the north atlantic and their global climate imprint. *Rev. Geophys.*, 42(1), 2004. ISSN 1944-9208. doi: 10.1029/2003RG000128. RG1005.
- I. J. Hewitt. Seasonal changes in ice sheet motion due to melt water lubrication. *Earth Planet. Sci. Lett.*,
355 371:16–25, 2013. doi: 10.1016/j.epsl.2013.04.022.
- C. L. Hulbe. An ice shelf mechanism for Heinrich layer production. *Paleoceanogr. Paleoclimatol.*, 12(5):
711–717, 1997. doi: 10.1029/97PA02014.
- C. L. Hulbe and M. Fahnestock. Century-scale discharge stagnation and reactivation of the Ross ice streams,
West Antarctica. *J. Geophys. Res.*, 112(F3), 2007. doi: 10.1029/2006JF000603.
- 360 C. L. Hulbe, D. R. MacAyeal, G. H. Denton, J. Kleman, and T. V. Lowell. Catastrophic ice shelf
breakup as the source of Heinrich event icebergs. *Paleoceanogr. Paleoclimatol.*, 19(1), 2004. doi:
10.1029/2003PA000890.
- N. R. Iverson, T. S. Hooyer, and R. V. V. Baker. Ring-shear studies of till deformation: Coulomb-
plastic behavior and distributed strain in glacier beds. *J. Glaciol.*, 44(148):634–642, 1998. doi:
365 10.3198/1998JoG44-148-634-642.
- G. Laske and G. Masters. A global digital map of sediment thickness. *Eos Trans. AGU*, 78:F483, 1997.
- B. P. Lipovsky, C. R. Meyer, L. K. Zoet, C. McCarthy, D. D. Hansen, A. W. Rempel, and F. Gimbert. Glacier
sliding, seismicity and sediment entrainment. *Ann. Glaciol.*, pages 1–11, 2019. doi: 10.1017/aog.2019.24.
- D. R. MacAyeal. A low-order model of growth/purge oscillations of the Laurentide Ice Sheet. *Paleoceanogr.*
370 *Paleoclimatol.*, 8(6):767–773, 1993a. doi: 10.1029/93PA02201.
- D. R. MacAyeal. Binge/purge oscillations of the Laurentide Ice Sheet as a cause of the North Atlantic’s
Heinrich events. *Paleoceanogr. Paleoclimatol.*, 8(6):775–784, 1993b. doi: 10.1029/93PA02200.
- E. Mantelli, M. B. Bertagni, and L. Ridolfi. Stochastic ice stream dynamics. *Proc. Natl. Acad. Sci.*, 113(32):
E4594–E4600, 2016. ISSN 0027-8424. doi: 10.1073/pnas.1600362113.
- 375 S. A. Marcott, P. U. Clark, L. Padman, G. P. Klinkhammer, S. R. Springer, Z. Liu, B. L. Otto-Bliesner,
A. E. Carlson, A. Ungerer, J. Padman, F. He, J. Cheng, and A. Schmittner. Ice-shelf collapse from
subsurface warming as a trigger for Heinrich events. *Proc. Natl. Acad. Sci.*, 108(33):13415–13419, 2011.
doi: 10.1073/pnas.1104772108.
- C. R. Meyer and I. J. Hewitt. A continuum model for meltwater flow through compacting snow. *Cryosphere*,
380 11(6):2799–2813, 2017. doi: 10.5194/tc-11-2799-2017.
- C. R. Meyer, A. S. Downey, and A. W. Rempel. Freeze-on limits bed strength beneath sliding glaciers. *Nat.*
Commun., 9(1):3242, 2018. doi: 10.1038/s41467-018-05716-1.
- B. Minchew, M. Simons, H. Björnsson, F. Pálsson, M. Morlighem, H. Seroussi, E. Larour, and S. Hensley.
Plastic bed beneath Hofsjökull ice cap, central Iceland, and the sensitivity of ice flow to surface meltwater
385 flux. *J. Glaciol.*, 62(231):147–158, 2016. doi: 10.1017/jog.2016.26.
- P. L. Moore. Deformation of debris-ice mixtures. *Rev. Geophys.*, 52(3):435–467, 2014. doi: 10.1002/
2014RG000453.

- K. O'Neill and R. D. Miller. Exploration of a rigid ice model of frost heave. *Water Resour. Res.*, 21(3): 281–296, 1985. doi: 10.1029/WR021i003p00281.
- 390 A. W. Rempel. Formation of ice lenses and frost heave. *J. Geophys. Res.*, 112(F2), 2007. doi: 10.1029/2006JF000525.
- A. W. Rempel. A theory for ice-till interactions and sediment entrainment beneath glaciers. *J. Geophys. Res.*, 113(F1), 2008. ISSN 2156-2202. doi: 10.1029/2007JF000870. F01013.
- A. W. Rempel. Frost heave. *J. Glaciol.*, 56(200):1122–1128, 2010. doi: 10.3189/002214311796406149.
- 395 A. W. Rempel. Hydromechanical processes in freezing soils. *Vadose Zone J.*, 11(4), 2012. doi: 10.2136/vzj2012.0045.
- A. W. Rempel and C. R. Meyer. Premelting increases the rate of regelation by an order of magnitude. *J. Glaciol.*, pages 1–4, 2019. doi: 10.1017/jog.2019.33.
- A. W. Rempel and M. G. Worster. The interaction between a particle and an advancing solidification front. *J. Cryst. Growth*, 205(3):427–440, 1999. doi: 10.1016/S0022-0248(99)00290-0.
- 400 A. W. Rempel, J. S. Wettlaufer, and M. G. Worster. Interfacial premelting and the thermomolecular force: Thermodynamic buoyancy. *Phys. Rev. Lett.*, 87(8):088501, 2001. doi: 10.1103/PhysRevLett.87.088501.
- A. W. Rempel, J. S. Wettlaufer, and M. G. Worster. Premelting dynamics in a continuum model of frost heave. *J. Fluid Mech.*, 498:227–244, 2004. doi: 10.1017/S0022112003006761.
- 405 A. A. Robel, E. DeGiuli, C. Schoof, and E. Tziperman. Dynamics of ice stream temporal variability: Modes, scales, and hysteresis. *J. Geophys. Res.*, 118(2):925–936, 2013. doi: 10.1002/jgrf.20072.
- S. Tulaczyk, B. Kamb, and H. F. Engelhardt. Basal mechanics of Ice Stream B, West Antarctica: 2. undrained plastic bed model. *J. Geophys. Res.*, 105(B1):483–494, 2000a. doi: 10.1029/1999jb900328.
- S. Tulaczyk, W. B. Kamb, and H. F. Engelhardt. Basal mechanics of Ice Stream B, West Antarctica: 1. till
410 mechanics. *J. Geophys. Res.*, 105(B1):463–481, 2000b. doi: 10.1029/1999JB900329.
- T. J. W. Wagner, R. W. Dell, I. Eisenman, R. F. Keeling, L. Padman, and J. P. Severinghaus. Wave inhibition by sea ice enables trans-atlantic ice rafting of debris during heinrich events. *Earth Planet. Sci. Lett.*, 495:157–163, 2018. ISSN 0012-821X. doi: 10.1016/j.epsl.2018.05.006.
- M. A. Werder, I. J. Hewitt, C. Schoof, and G. E. Flowers. Modeling channelized and distributed subglacial
415 drainage in two dimensions. *J. Geophys. Res.*, 118(F20146):1–19, 2013. doi: 10.1002/jgrf.20146.
- J. S. Wettlaufer and M. G. Worster. Premelting dynamics. *Annu. Rev. Fluid Mech.*, 38(1):427–452, 2006. doi: 10.1146/annurev.fluid.37.061903.175758.
- M. G. Worster. Solidification of fluids. In G. K. Batchelor, H. K. Moffatt, and M. G. Worster, editors, *Perspectives in Fluid Dynamics*, chapter 8, pages 393–444. Cambridge University Press, 2000.
- 420 F. A. Ziemer, M.-L. Kapsch, M. Klockmann, and U. Mikolajewicz. Heinrich events show two-stage climate response in transient glacial simulations. *Clim. Past*, 15(1):153–168, 2019. doi: 10.5194/cp-15-153-2019.